

Design of a Hybrid Ambient Low Frequency, Low Intensity Vibration Energy Scavenger

M. Khbeis^{1,2}, J. McGee¹, C. Richardson², and R. Ghodssi^{1*}

¹MEMS Sensors and Actuators Laboratory (MSAL), Department of Electrical and Computer Engineering,
Institute for Systems Research, University of Maryland, College Park, MD 20742, U.S.A.

²Laboratory for Physical Sciences

8050 Greenmead Drive, College Park, MD 20740, U.S.A.

Tel: 301-405-8158; Fax: 301-314-9281; Email: ghodssi@eng.umd.edu

Abstract

We report, for the first time, the design of a hybrid ambient low frequency, low intensity vibration energy scavenger (HALF-LIVES) that simultaneously couples both piezoelectric and electrostatic transduction mechanisms. A systematic design approach results in a simulated power density of $1.17\mu\text{W}/\text{mm}^3$ with input accelerations of $1\text{m}/\text{s}^2$ at 120Hz. This power density estimation is achieved by optimizing various mechanical components of the system through analytical and numerical modeling while minimizing control losses. A system overview, dynamic model and control circuitry are presented.

Keywords: Energy scavenging, vibration, hybrid design, piezoelectric, electrostatic

1 – INTRODUCTION

Recently, significant interest in providing long-term energy for autonomous wireless sensor networks has driven development of both piezoelectric and electrostatic vibration energy scavengers [1]. However, while research to date has shown macroscopic examples of energy harvesting devices, the capability to provide usable energy does not scale well as harvester dimensions are reduced.

An ambitious research program in minute sensor networks, commonly referred to as Smart Dust, has a specified final system volume of less than 25mm^3 per node. For this sensor network, mechanical energy conversion is expected to be too low to power communications between nodes, forcing a reliance on active power via a rectenna using an externally applied radio frequency (RF) power source [2]. However, assuming the RF source is intermittent and has a very low duty cycle, a secondary source of energy is required to maintain sensing in addition to microprocessor state logic and event storage operations.

Given the volumetric limitations, the optimum energy conversion requires a system that maximizes the amount of energy conversion while simultaneously minimizing the energy consumption of the control electronics and power conditioning circuits. For the first time, this paper presents a system-based design of a hybrid ambient low frequency, low intensity vibration energy scavenger (HALF-LIVES).

2 – HALF-LIVES SYSTEM OVERVIEW

Several electrostatic scavenger architectures have been presented; however, the active control systems for timing the charge and discharge cycles can consume significant amounts of scavenged energy [3]. Recently, diode connections and flyback circuits have been utilized to reduce the amount of control required for charge constrained energy conversion [4],[5]. However, these asynchronous systems still require a source for pre-charging the variable capacitor. In the hybrid vibration harvester, the goal is to provide a standalone method of generating pre-charge while providing precise, synchronous charge control with low energy consumption.

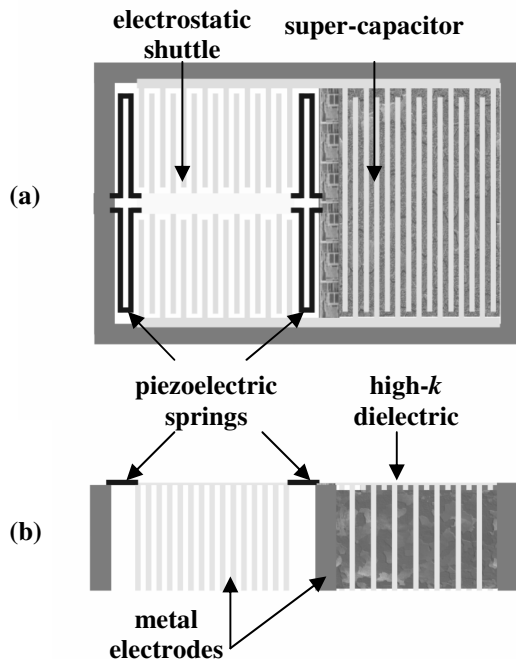


Figure 1 – Concept drawing of HALF-LIVES system:
(a) top view (b) schematic cross section view

Energy conversion components of the hybrid vibration scavenger are an electrostatic oscillator, doubling as a proof mass, that is suspended by several piezoelectric springs as depicted in Fig. 1. As depicted in the system diagram shown in Fig. 2, the piezoelectric components concurrently provide an input voltage to a full wave rectifier to provide a DC power rail (VDD) and to a simple peak detector to provide control signals for gating the charge and discharge times. The control signals pre-charge the variable capacitor structure to VDD that performs charge constrained conversion and subsequently supplies scavenged energy to the supercapacitor. Due to the complexity of this system, a comprehensive analytical model describing the dynamic behavior of the system is required.

3 – ANALYTICAL MODEL

While some aspects can be modeled through finite element analysis (FEA), the true dynamic interactions between mechanical and electrical components are only realized via a comprehensive analytical model.

3.1 – Generic Scavenger Model

The William and Yates original generic vibration harvester model of a spring, mass, dash-pot system that is expanded by Roundy *et al*, represents the system at the highest level and is defined by Eq. (1) [1],[6].

$$-m\ddot{x} = m\ddot{y} + f_e(\dot{y}) + f_m(\dot{y}) + ky \quad (1)$$

In Eq.(1), x is the input displacement, y is the internal displacement, m is the mass, k is the spring constant, and $f_e(\dot{y})$ and $f_m(\dot{y})$ are the electrical and mechanical loss functions respectively. For this system, the loss functions must simultaneously incorporate all loss mechanisms of both piezoelectric and electrostatic components.

3.2 – Piezoelectric Spring Model

Simple folded piezoelectric elements play a dual role as the mechanical springs and electrical pre-charge and control signals. A simple 3-dimensional (3-D) mechanical model is needed to determine the 3-D displacement and associated stress within the bending element. Steward provides a detailed application of Castigliano's 2nd theorem and internal strain energies to determine the displacement of the spring element due to movement of a proof mass by an applied force [7]. The bending stress in the plane of the spring is approximated by considering the Euler-Bernoulli beam equation and axial strain along the beam, resulting in Eq. (2), where F_x is the axial force, M_y and M_z are the bending moments, y and z are the width and height from the beam neutral axis, A is the cross-sectional area, and I_y and I_z are the second moments of area.

$$\sigma_x(x, y, z) = \frac{F_x(x)}{A} + \frac{M_y(x)z}{I_y} + \frac{M_z(x)y}{I_z} \quad (2)$$

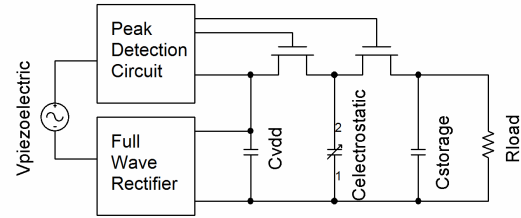


Figure 2 – Hybrid scavenger system diagram

The sum of the integrals of Eq. (2) along each element of the folded spring determines average principle stress. This value closely approximates the von Mises stress calculated by FEA. However, it should be noted that the average stress represents the effects of a piezoelectric bender covered completely by a single pair of electrodes and thus the peak stresses cancel. In reality, electrode placement is optimized to extract the localized induced voltage. Using FEA modeling, a ratio of localized peak stress to average stress provides a stress multiplication factor of the input stress to the electromechanical piezoelectric transformer model. The piezoelectric basic transformer model that translates mechanical energy, on the left side of the transformer, to electrical has been well documented and is illustrated in Fig. 3(a) [1].

The piezoelectric mechanical loss components are inertial, mechanical damping, and stiffness represented by the inductor, resistor, and capacitor respectively. In addition, the mechanical and electrical loss mechanisms of the electrostatic module are included where appropriate.

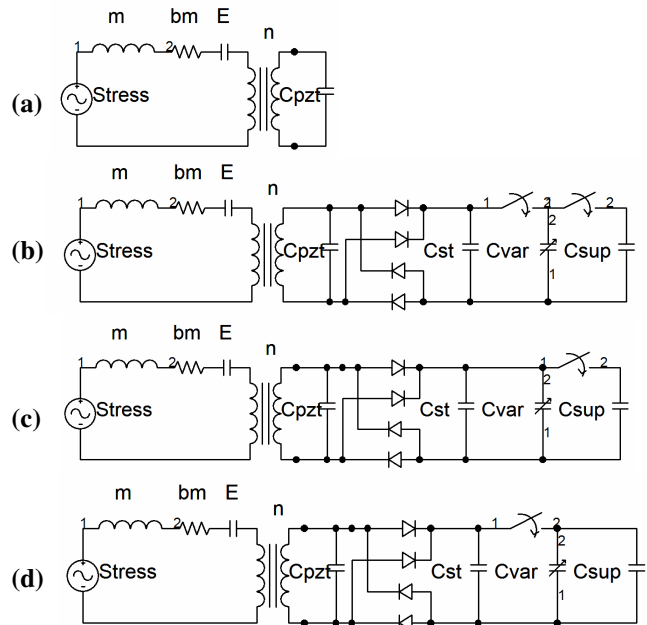


Figure 3 – Stages of scavenging operation: (a) piezoelectric elements disconnected, (b) full-wave rectified voltage charging temporary storage capacitor, (c) charge transfer to variable capacitor at C_{max} , (d) charge transfer from variable capacitor to supercapacitor at C_{min}

3.3 – Electrostatic Conversion Model

The electrostatic module is comprised of a proof mass shuttle with interdigitated electrodes that creates a variable capacitor. A charge constrained model is widely used for electrostatic energy conversion with the energy transfer per half cycle defined in Eq. (3) [3],[4],[5].

$$\Delta E = \frac{1}{2} V_{IN} V_{OUT} (C_{max} - C_{min}) \quad (3)$$

Ideally, the system pre-charges a temporary storage capacitor as shown in Fig.3(b). Figure 3(c) illustrates the charge transfer from the temporary storage capacitor to the variable capacitor at the maximum displacement resulting in a fixed charge and discharges at the neutral point, resulting in a large V_{OUT} that is applied to a supercapacitor as illustrated in Fig. 3(d).

Numerous methods have been attempted to synchronize or circumnavigate the charge cycle timing; however, in this system the piezoelectric voltage derivative is monitored to observe peaks and neutral points using simple control electronics. The control is modeled by monitoring the zeros and extrema of the voltage derivative to define charge and discharge times respectively.

For the HALF-LIVES system to be effective, every effort must be made to scavenge the maximum amount of energy. Typically, mechanical stops are used to prevent shorting of the electrodes. Due to fabrication limitations the minimum feature size for these mechanical stops is generally on the order of several microns, the maximum capacitance and thus charge is limited as shown in Eq. (4), where N_g is the number of gaps, κ is the dielectric constant of air, ϵ_0 is the free space permittivity, L_o is the length of electrode overlap, h is the height, d is the initial gap and w_{stop} is the width of the mechanical stop.

$$C_{max} = 2N_g \kappa \epsilon_0 L_o h \left(\frac{d}{2dw_{stop} - w_{stop}^2} \right) \quad (4)$$

Microfabrication of supercapacitors, using high- k dielectrics is an application that is being co-developed in conjunction with the hybrid scavenger. Using this fabrication technology, a sub-micron dielectric coating can be used to prevent shorting while decreasing the gap between electrodes, resulting in an increased maximum capacitance as defined in Eq. (5), where κ is the dielectric constant and w_d is the thickness of the insulating coating. This increase in capacitance is 2 to 10 times larger than the alternative given a mechanical stop of 1 micron.

$$C_{max} = N_g \epsilon_0 L_o h \left(\frac{1}{\frac{2w_d}{\kappa}} + \frac{1}{2d + 2w_d \left(\frac{1 - 2\kappa}{\kappa} \right)} \right) \quad (5)$$

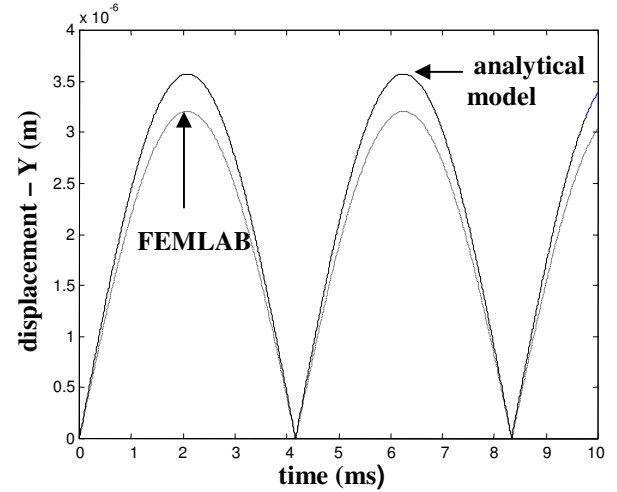


Figure 4 – Comparison of FEMLAB simulation to analytical model for displacement in primary (Y) axis.

4 – FINITE ELEMENT COMPARISON

To ensure accuracy of the implementation of the analytical mechanical model in MATLAB results were compared with finite element analysis (FEA) in FEMLAB. Figure 4 demonstrates a close correlation between the dynamic analytical model and FEA displacement output. At 2.5 microns of displacement, FEA outputs for peak von Mises stress is 0.457 GPa versus model value of 0.475 GPa.

5 – PRELIMINARY MODELING RESULTS

The analytic model was implemented in MATLAB using the parameter values in Table 1. Excitation is a $1m/s^2$ sinusoidal acceleration at a frequency of 120 Hz. The simulation was run for 15 seconds, with a steady state half cycle energy transfer of 58.3 nJ. This results in a power delivery of 14 μW and an initial power density of 1.17 $\mu W/mm^3$. Optimized design parameters are extracted by sweeping multiple parameters to maximize energy transfer as depicted in the sample sweep in Figure 5. Once these parameters are defined, the spring dimensions and circuit component values will be used in fabrication and test of the system.

Table 1 – Initial model design parameters

Parameter	Value	Parameter	Value
num springs	4	Num gaps	312
Spr length	500e-6 m	Elec length	2.3e-3 m
Spr width	20e-6 m	Elec width	20e-6 m
Spr height	8e-6 m	Elec height	500e-6 m
Material	PZT-502	Material	Gold
$\kappa_{pzt-502}$	1730	Density	19320 kg/m ³
$E_{pzt-502}$	7.1e10	Initial gap	6e-6 m
Poisson ratio	0.31	Cstore	1e-3 F
d_{31}	-175e-12	Csupercap	1e-3 F
Power	14μW	Pwr Density	1.17 $\mu W/mm^3$

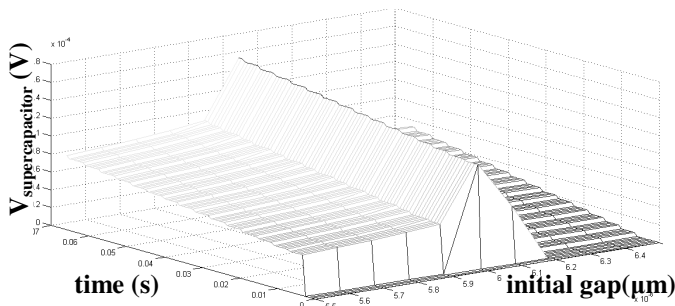


Figure 5 – Parametric sweep in MATLAB model

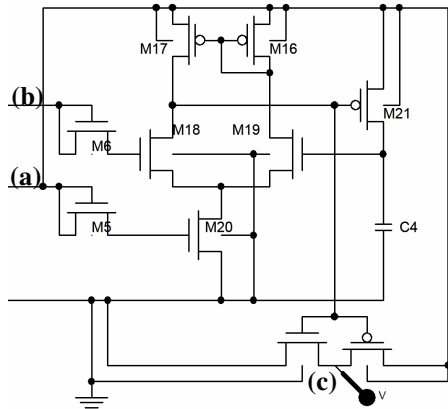


Figure 6 – Peak detector circuit: (a) VDD, (b) full wave rectified, and (c) charge control output

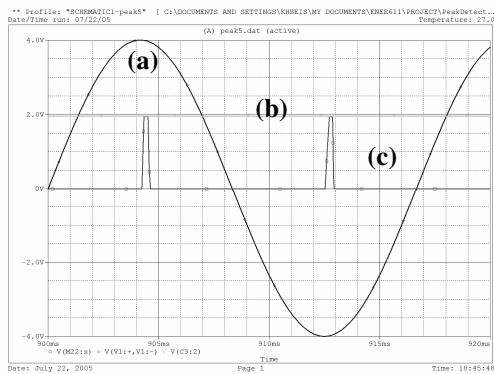


Figure 7 – PSpice simulation: (a) piezoelectric input voltage, (b) VDD, and (c) charge control signal

6 – CONTROL ELECTRONICS

The control electronics for detection of a voltage peak or zero voltage are quite simple. As shown in Fig. 6, the peak detector circuit employs a simple differential pair with a feedback capacitor and PMOS gate. The peak detection circuit output is fed into an inverter pair for supplying a buffered charge control pulse at the piezoelectric voltage extrema as shown in Fig. 7. A second detector circuit is necessary to detect the neutral (zero voltage) condition. PSPICE simulations show that the peak power consumption of each charge control circuit is approximately 200nW. It should be noted that detection

operation can be interrupted if the reference capacitor (C4) saturates; therefore it may be necessary to bleed charge regularly, increasing losses slightly.

7 – FUTURE WORK

Currently the electrostatic proof mass is being fabricated and suitable piezoelectric materials are being investigated. Fabrication limitations in processes will be applied to the model to finalize geometries. Once the initial system is fabricated, validation of the analytical model will be performed.

8 – CONCLUSIONS

An analytical model for describing dynamic behavior of a hybrid piezoelectric and electrostatic vibration harvester is presented. A simple electrical circuit utilizing piezoelectric voltage signals to perform charge control while additional spring elements provide the pre-charge and rail voltages. Fabrication development and a closed-loop design using the model are underway.

ACKNOWLEDGEMENTS

The authors wish to express sincere gratitude to the Laboratory for Physical Sciences for funding support, members of the MEMS Sensors and Actuators Laboratory (MSAL) for providing constructive feedback, and LPS cleanroom management for fabrication support.

REFERENCES

- [1] S. Roundy *et al*, *Energy Scavenging for Wireless Sensor Networks with Special Focus on Vibrations*, Kluwer Academic Publishers 2004.
- [2] M. Ghovanloo and K. Najafi, "Fully integrated power supply design for wireless biomedical implants," *2nd Annual Int'l IEEE-EMBS Special Topic Conf. on Microtechnologies in Medicine & Biology.*, USA 2002.
- [3] S. Meninger *et al*, "Vibration-to-electric energy conversion," *IEEE Transactions on VLSI Systems*, vol. 9, pp. 64-76, 2001.
- [4] G. Despesse *et al*, "Design and fabrication of a new system for vibration energy harvesting," *2005 PhD Research in Microelectronics and Electronics*, vol. 1, pp. 225-228, 2005.
- [5] B. Yen and J. Lang, "A variable capacitance vibration-to-electric energy harvester," *IEEE Transactions on Circuits and Systems I: Fund. Theory and Applications*, vol. 53, pp. 288-295, 2006.
- [6] C. B. Williams and R.B Yates, "Analysis of a microelectric generator for microsystems", *Proc. Transducers 95/Euroensors IX*, 369-372, 1995.
- [7] V. Steward, "Modeling of a folded spring supporting MEMS gyroscope", Master of Science at the Worcester Polytechnic Institute, 2003.